Inter- or Intramolecular N···H−O or N−H···O Hydrogen Bonding in 1,3-Amino-α/β-naphthols: An Experimental NMR and Computational Study

Anica Lämmermann,[†] István Szatmári,[‡] Ferenc Fülöp,[‡] and Erich Kleinpeter*,[†]

Department of Chemistry, University of Potsdam, Karl-Liebknecht-Str. 24-25, 14476 Potsdam(Golm), Germany, and the Research Group for Stereochemistry, Hungarian Academy of Sciences-Institute of Pharmaceutical Chemistry, University of Szeged, Eötvös u. 6., H-6720 Szeged, Hungary

Received: March 26, 2009; Revised Manuscript Received: April 8, 2009

The existence of intermolecular or intramolecular N···H−O or N−H···O hydrogen bonding in three series (series **1**, substituted 1-aminoalkyl-2-naphthols: R = H, Me, Et, Pr, *i*-Pr; series **2**, substituted 1-α-aminobenzyl-2-naphthols: H, *p*-OMe, *p*-F, *p*-Cl, *p*-Br, *p*-NO_2, *p*-Me; series **3**, substituted 2-α-aminobenzyl-1-naphthols: R = H, *p*-Me, *p*-F, *p*-Br, *p*-OMe, *m*-NO_2, *m*-Br) are studied by NMR spectroscopy and computed at the DFT level of theory [B3LYP/6-311+G(d,p)]. The correct nature of the H-bond was assigned unequivocally both experimentally and computationally by potential energy scans rotating the involved dihedral angles. We investigated the effects of substituents on the strength of the H-bond by evaluating the corresponding hyperconjugative stabilization energy $n_{\text{lonepair}} \rightarrow \sigma^*_{\text{X−H}}$ and Hammett substituent constant plots. By this means, steric and electronic substituent effects could be easily quantified and separated.

1. Introduction

Hydrogen bonds (H-bonds) are very important interactions in a wide range of chemical and biological systems (e.g., RNA, protein folding, and crystal engineering). They stabilize secondary and tertiary structures of many biomolecules and maintain the conformations necessary for the chemical functionality of flexible macromolecules.[1] The double helix structure of DNA especially depends on the presence of H-bonds between the strands. Possible H-bonds in transition-state structures may also govern the conformation of the excited state of chemical reactions and thereby the whole reaction pathway.[2] H-bonds are of particular importance for anion-binding processes because they enhance the ability of receptor species to act as transport agents for anions across biological membranes, which is of intense current interest.[3]

The strength of a H-bond strongly depends on both the relative orientation of the acceptor X−H bond to the lone pair of the donor Y and the electrostatic strength of the acceptor−$H^{\delta+}\cdots^{\delta-}$Y dipole/dipole interaction. Almost linear H-bond X−H···Y geometry is the basis for α helices, β-sheet structures, and nucleic acid base pairs.[4]

Numerous experimental NMR, UV−vis, and IR spectroscopic investigations on H-bonding have been reported.[5−9] In ^{1}H NMR spectra, the presence of H-bonding is readily indicated by more-or-less broadened X−H signals and the low field position of the corresponding resonance; the stronger the H-bond, the lower field shifted the X−H signal. The δ values of X−H protons usually excellently correlate with the X−H···Y H-bond length; corresponding studies have recently been published on α-, β-, and γ-cyclodextrins.[10] Furthermore, hydrogen bonding was identified to be the main factor for preference of the eq,eq over ax,ax conformation in *trans*-2-halocyclohexanols.[11]

Another interesting aspect of studies on H-bonding is the adequate application and evaluation of the O−H coupling constants to vicinal C−H protons, which prove to be characteristically dependent on the orientation of the OH group; for example, Bernet et al.[12] characterized the H-bonding in fluorinated saccharides by utilizing the vicinal ^3J(H,OH) coupling constants.

If H-bonding is involved in chromophores of molecules, then experimental evidence can be obtained via electronic absorption or emission spectroscopy. Both blue and red shifts can occur depending on the strength and the position of the H-bonding. It has been observed experimentally that the corresponding electronic transitions are shifted in the blue direction when the chromophore is involved in H-bonding as the acceptor but are shifted in the red direction when it serves as the donor.[9]

Recently, well-established spectroscopic methods have been increasingly combined with parallel computational methods.[13] Besides computational structural studies for extracting global and local energy minima structures and the computation of NMR parameters, natural bond orbital (NBO) analysis[14] is currently playing an ever more significant role. The NBO analysis method involves population analysis, which distributes computed electron density to orbitals in the way in which chemists think in terms of physical organic chemistry. Furthermore, additional tools of NBO analysis compute the amounts of orbital interactions, stabilization energies caused by electron transfer, and hyperconjugation stabilization energies.

Considerations of hyperconjugative interactions are playing an ever greater role in the quantitative study of the nature of H-bonds.[2] Ducati et al. carried out a detailed investigation of the conformations of C=O and C=S compounds via NBO analysis;[15] by analyzing the hyperconjugative energies, they concluded that the C=S group exhibits a better proton acceptor capability than that of the C=O bond. De Oliveira and Rittner[16] scrutinized the importance of intramolecular H-bonding on 1,3-diaxial interactions of *cis*-3-alkoxycyclohexanols and the influence of the six-membered ring systems on the conformational equilibria. Therefore, by the combined

* Corresponding author. Tel: +49-331-977-5210. Fax: +49-331-977-5064. E-mail: kp@chem.uni-potsdam.de.
† University of Potsdam.
‡ University of Szeged.

10.1021/jp902731n CCC: $40.75
Published on Web 05/07/2009

application of NMR spectroscopy, IR spectroscopy, and accompanying DFT computations, they established that the strength of intramolecular H-bonds increases with increasing size and the upward inductive effect of the *cis*-3-alkoxy substituent.[16]

The compounds studied in this article are three different types of aminonaphthols as follows: 1-aminoalkyl-2-naphthols[17] (**1**, Figure 1), 1-α-aminobenzyl-2-naphthols (**2**),[18] and 2-α-aminobenzyl-1-naphthols (**3**).[19] These aminonaphthols exert biological activity against the $H_{37}D_v$ strain of *Mycobacterium tuberculosis* in vitro.[20] Such activity against bacteria and enzymes proves to be highly dependent on the active conformation of the molecules, which is strongly influenced by H-bonding. For this reason, we investigated compounds in series **1**−**3** with particular regard to the existence of inter/intramolecular H-bonding in the molecules. Additionally, there are substituents in the H-bond fragment X−H···Y with different steric and electronic effects that could influence both the strength and the steric requirements of H-bonding present and hence the overall molecular geometry of the compounds. Whereas steric substituent effects can be evaluated via the Meyer parameters, V^a,[21] the electronic substituent effects can be readily quantified via the Hammett substituent constants σ.[22,23]

2. Experimental Section

2.1. Synthesis and NMR Spectra of the Compounds Studied. The hydrochlorides of the compounds studied were prepared as previously described: **1a**−**1e**,[17] **2a**−**2g**,[18] and **3a**−**3g**.[19] These stable compounds were neutralized with 300−400 μL of 1 M NaOH, and residual acidic protons were quenched with pyridine. ^{1}H NMR spectra were recorded on 0.04 M L^{-1} solutions in $CDCl_3$ at 300.13 and 500.17 MHz using a 5 mm probe with TMS as the internal reference.

2.2. Theoretical Calculations. Potential energy surface scans were performed at the B3LYP/6-311+ G(d,p) level of theory by rotation of the dihedral angle C7−C1−C6−N5. Geometries were fully optimized with the program Gaussian 03[24] by employing the DFT theory at the B3LYP/6-311+G(d,p) level.[25−27] The hyperconjugation energies were calculated by using NBO analysis[14] (NBO 5.0), which is compiled in Gaussian 03.

With second-order perturbation theory analysis, it is possible to estimate donor−acceptor interactions. For each donor NBO (*i*) and acceptor NBO (*j*), the stabilization energy *E*(2) associated with delocalization $i \rightarrow j$ is estimated to be

$$E(2) = \Delta E_{ij} = q_i \frac{F(i,j)^2}{\varepsilon_j - \varepsilon_i} \quad (1)$$

where q_i is the donor orbital occupancy, ε_i and ε_j are diagonal elements (orbital energies), and $F(i, j)$ are the off-diagonal NBO Fock matrix elements.[28]

We calculated chemical shifts by the GIAO method[29] at the B3LYP/6-311+G(d,p) level of theory by subtracting the nuclear magnetic shielding tensors of protons in aminonaphthols **1**−**3** and tetramethylsilane (TMS) as a reference calculated at the same level of theory.

3. Results and Discussion

3.1. Experimental ^{1}H NMR Spectra. The resonances of the aromatic protons in the free amines **1**−**3** could be assigned as previously described for the corresponding hydrochlorides.[17−19] Therefore, the free aminonaphthols are stable, and the interesting OH/NH_2 protons were recorded separately at $\delta > 12$ (1 proton) and δ 2 to 3 (2 protons). The two signals were still more or less broadened beyond the paramagnetic line broadening because of the ^{14}N isotope; this auxiliary broadening differed from compound to compound; whereas the signals of the protons at δ 2 to 3, obviously the NH_2 protons, changed to only a minor extent, the line width of the OH proton at $\delta > 12$ varied from line widths similar to those for the NH_2 protons up to extremely broadened absorptions with line widths of >2 ppm. Consequently, both the OH and the NH_2 protons appeared to be involved in inter- and intramolecular H-bonding, and study of this issue will comprise the main topic of this article to ascertain the predominant structure that is biologically active against enzymes and bacteria.[20]

First, the temperature dependence of the ^{1}H chemical shifts and line widths of the OH/NH_2 signals in the ^{1}H NMR spectra of **1**−**3** were studied with the following results: (i) The proton signal of the NH_2 amino protons changed only very slightly ($\Delta\delta = 0.02$ in **2a**) when the solution was cooled to −80 °C; the line width of the signal remained almost constant, and there was not the slightest hint of splitting of the signal. (In the case of an intramolecular H-bond, the corresponding low-field N−H signal and another remaining NH signal would be expected.) (ii) The OH proton was strongly low-field shifted ($\Delta\delta/\Delta T =$ 6.8 ppb in **2a**) when the temperature was lowered to −80 °C in CD_2Cl_2; a strictly linear dependence was observed. Moreover, upon going to lower temperatures, the line width dramatically improved; at −80 °C, normal high-resolution line widths of <1 Hz were seen. For example, in Figure 2, both the ^{1}H chemical

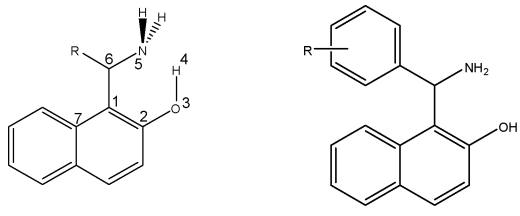

1

2

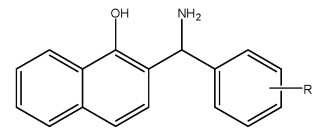

3

Compound	Substituent (R)	Compound	Substituent (R)	Compound	Substituent (R)
1a	H	**2a**	*p*-NO_2	**3a**	*p*-Me
1b	Et	**2b**	*p*-Cl	**3b**	*m*-NO_2
1c	*i*-Pr	**2c**	*p*-OMe	**3c**	*m*-Br
1d	Pr	**2d**	*p*-Br	**3d**	*p*-Br
1e	Me	**2e**	H	**3e**	*p*-F
		2f	*p*-F	**3f**	H
		2g	*p*-Me	**3g**	*p*-OMe

Figure 1. Aminoalkyl α- and β-napthols investigated.

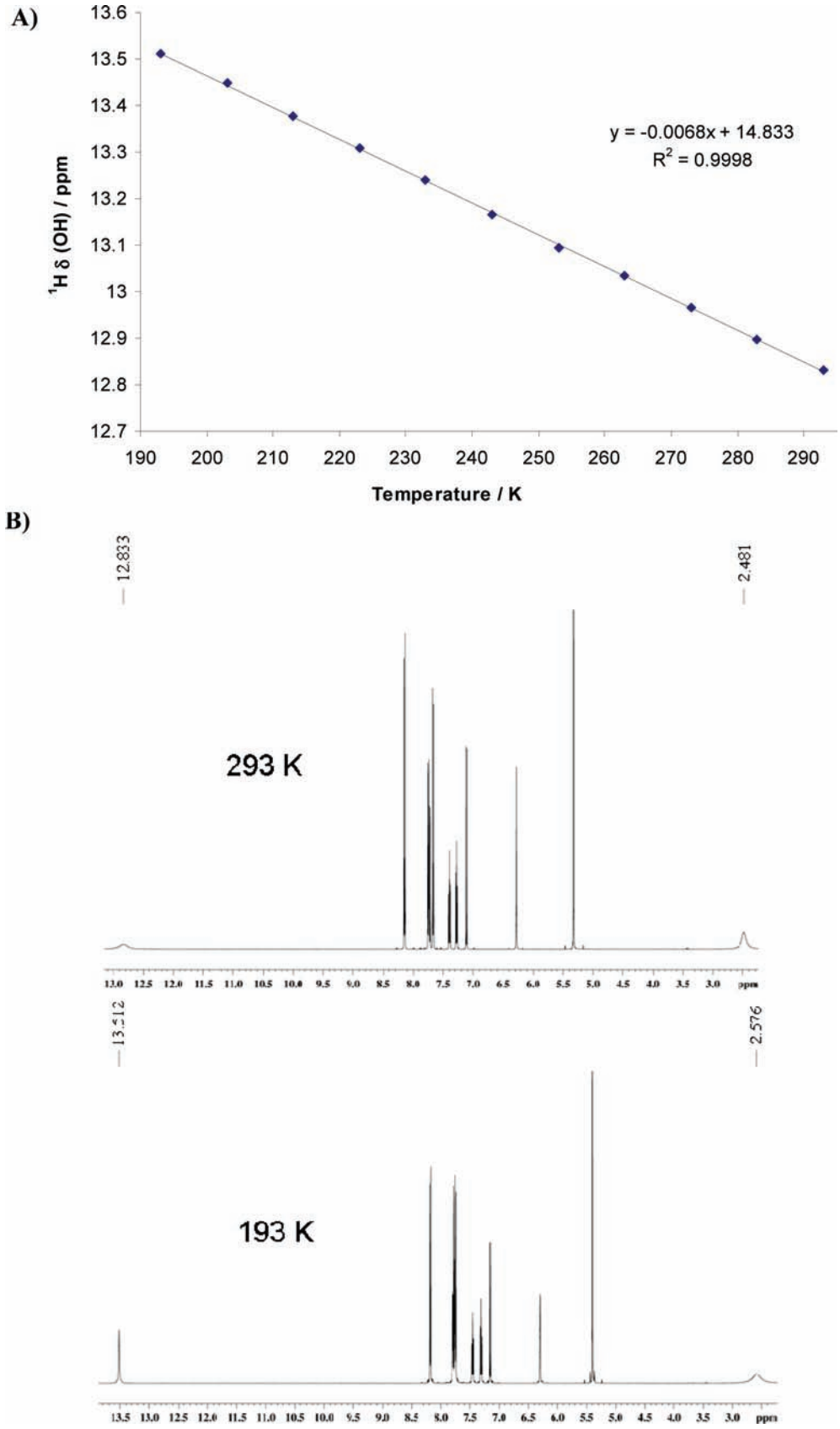

Figure 2. (A) Temperature dependence of the OH proton ($\Delta\delta/\Delta T = -6.8$ ppb; regression coefficient given) and (B) ^{1}H NMR spectrum of **2a** at room temperature and at 193 K (in CD_2Cl_2).

shift dependence of the OH proton and the ^{1}H NMR spectrum at ambient temperature and at −80 °C of compound **2a** in CD_2Cl_2 are given. (iii) Furthermore, there was only one OH signal at lower field at −80 °C. If the OH proton were both inter- and intramolecularly bonded, then two signals would be expected. The quotient obtained (e.g., $\Delta\delta/\Delta T = 6.8$ ppb in **2a**) compared with the submitted temperature quotients[30−34] was between the characteristic ranges expected for intra- ($\Delta\delta/\Delta T <$

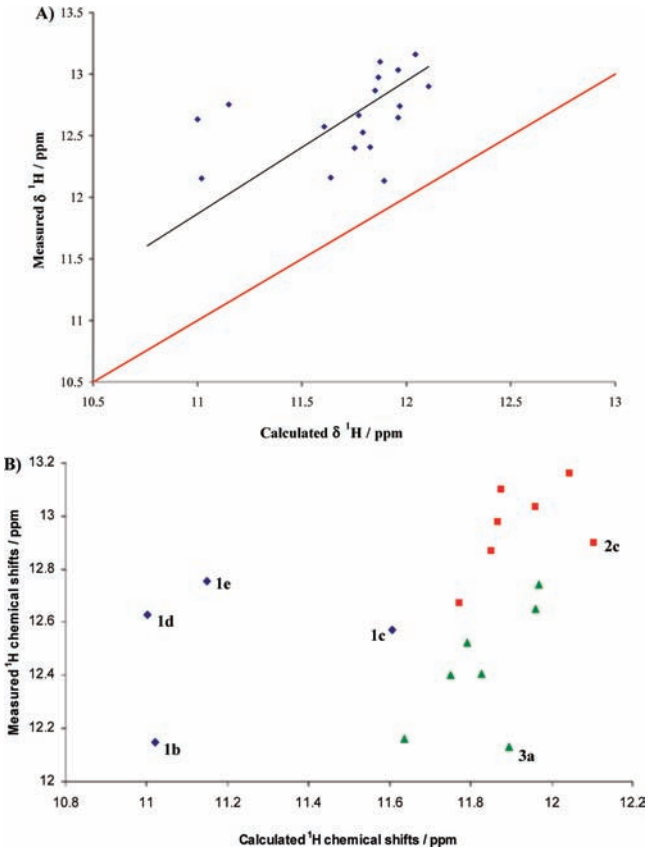

Figure 3. Correlation of experimental and computed ^{1}H chemical shifts of the OH proton: (A) general and (B) ordered for series **1** (◆), **2** (■), and **3** (▲).

4 ppb) and intermolecular H-bonds ($\Delta\delta/\Delta T > 7$ to 8 ppb) with OH as proton donors. However, the structures studied previously are not really comparable to the present compounds **1**−**3**. From the experiments and the computations seen below, intramolecular O−H···N bonding was concluded (vide infra). (iv) The concentration dependences of the two OH/NH_2 signals were also investigated: the chemical shifts were not dependent on the concentration of the CD_2Cl_2 solution.

Initially, therefore, the computed chemical shifts of the OH proton, fixed in intramolecular H-bonding with OH as the proton donor and the nitrogen lone pair as acceptor (O−H···N), were correlated to the experimental values; the corresponding correlation (given in Figure 3a), including all molecules **1**−**3**, obviously makes no sense. However, if the molecules are readjusted to the three different structures **1**, **2**, and **3**, then the situation improves (cf. Figure 3b): For the naphthols **2** and **3**, acceptable linear dependences were obtained (with **2c** and **3a**, respectively, as outliers); for the β-naphthols **1**, no reasonable correlation was observed. Because of possible peri interactions of substituent R and β-naphthol moiety in series **1**, distortionless generation of intramolecular hydrogen bonding hardly suffers from substituent volume and, in addition, the solvent was not considered along computations; obviously, this is a borderline case for still employing theoretical calculations. The situation improves for aminonaphthols **2** and **3**; significant correlations were obtained and corroborate the suggestion of O−H···N H-bonding in the compounds studied. Structural changes along series **2** and **3** are not of steric influence on the intramolecular H-bond, and the same dependence on electronic substituent effects (same slopes) has been found. The dependences are tendencies only, but when considering that the OH protons were

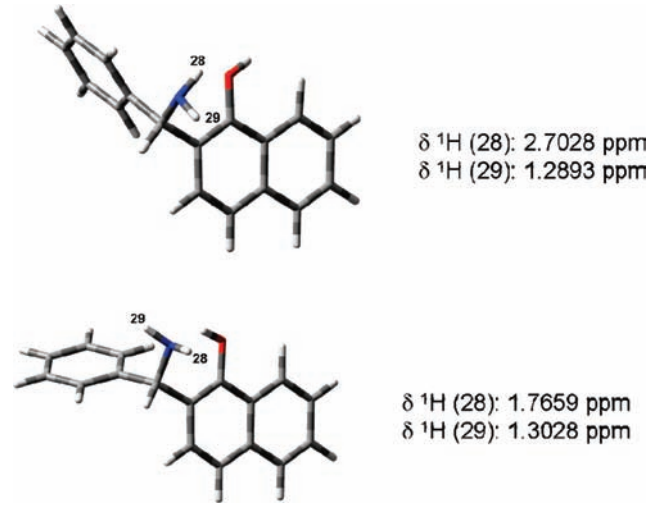

Figure 4. Computed ^{1}H chemical shifts of the NH_2 protons in the two possible intramolecular H-bonds.

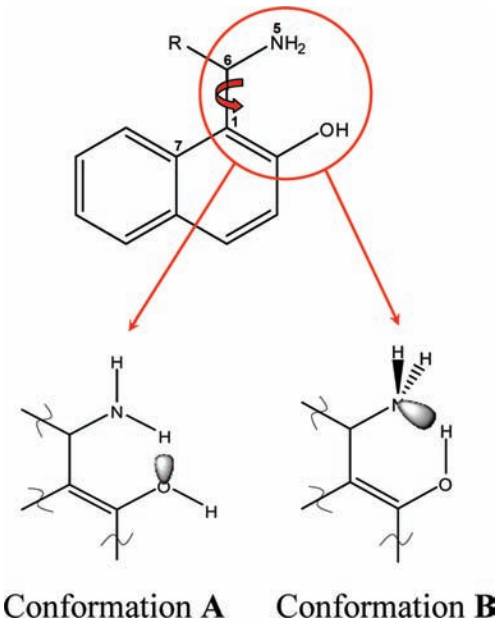

Figure 5. Two possible orientations for intramolecular H-bonding in **1**−**3**: (A) one N−H bond to the OH group oxygen as electron donor and (B) O−H bond to the nitrogen lone pair as electron donor.

studied theoretically, this is robust information for the presence of intramolecular O−H···N hydrogen bonding. For the alternative H-bond with N−H as proton donor and the oxygen lone pair as acceptor, N−H···O, different chemical shifts for the N−H protons at significantly higher field (cf. Figure 4) were computed.

3.2. Nature of Intramolecular H-Bonding and Search for Global Minimum Structures. To detect the global minima structures of **1**−**3**, we processed potential energy scans by changing the C7−C1−C6−N5 dihedral angle stepwise; the position of the single absorption at around δ 12 prompted us to study first the O−H···N intramolecular H-bonding, but, as mentioned already, two different intramolecular H-bonds are accessible in **1**−**3**: the O−H···N lone pair and the N−H···O lone pair (cf. Figure 5). The results of the corresponding computations by varying the C7−C1−C6−N5 dihedral angle stepwise are given in Figure 6; the oxygen is the donor atom in conformation **A**, whereas that in conformation **B** is the lone pair on the nitrogen. To investigate which conformation is more

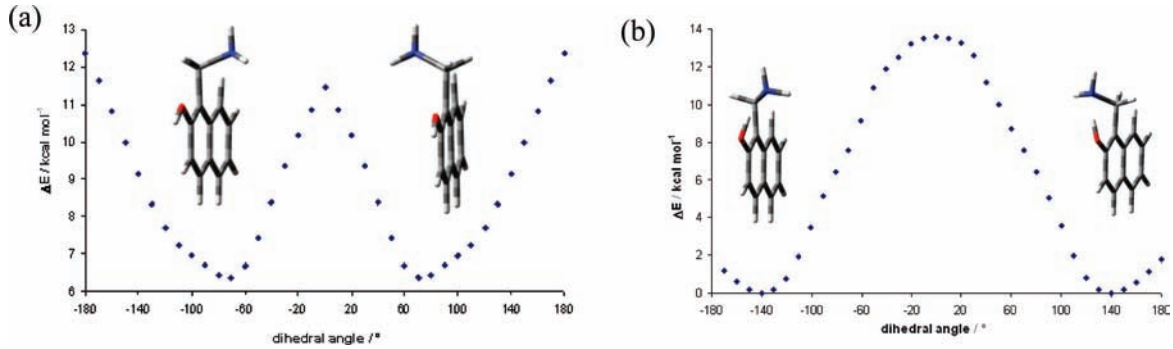

Figure 6. Potential energy scans relating to the torsion angle C7−C1−C6−N5 in **1a**: (a) oxygen lone pair as donor and (b) nitrogen lone pair as donor.

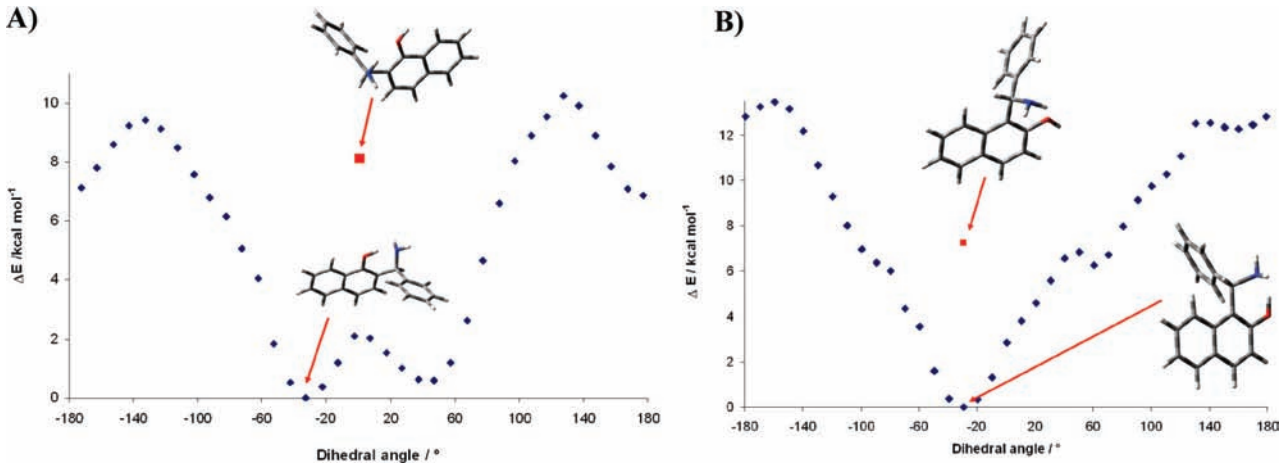

Figure 7. Potential energy scans relating to the dihedral angle C7−C1−C6−N5 in (A) **3f** and (B) **2e** (◆); energy-optimized geometry of the N−H···O H-bond structure (■) at comparable dihedral angles.

favorable, the dihedral angel C7−C1−C6−N5 for the two possibilities of intramolecular H-bonding was varied from 10 to 360°, and for each step the obtained geometry was energy-optimized.

The potential energy scans obtained (cf. Figure 6) for the two cases of intramolecular H-bonding provide two identical local energy minima **A** with a H-bond distance of 2.32 Å (Figure 6a); intramolecular H-bonding was not found. For conformation **B**, two global minima structures were again obtained (cf. Figure 6b), but with an intramolecular H-bond (O−H···N distance 1.80 Å); these structures are 6.4 kcal mol^{-1} more stable than the corresponding energy minimum structures of conformation **A**.

Therefore, it can be concluded unequivocally from the computations (and this in agreement with the experimental NMR studies) that in the Betti base derivatives **1**−**3**, the lone pair of the NH_2 group acts as the electron donor and the OH oxygen as the acceptor unit of the intramolecular H-bond O−H···N; identical results were obtained for the corresponding phenyl-substituted analogues **2** and **3** (cf. Figure 7).

3.3. Geometry of the O−H···N H-Bond in 1−3. Selected geometry parameters for compounds **1**−**3** computed at the DFT level of theory are listed in Table 1. The intramolecular H-bond influences several bond angles and bond lengths; notable differences are observed. Significant linear dependences on the properties of the various substituents in **1**−**3** were often detected.

The shorter the OH···N H-bond, the larger the corresponding computed O−H bond: the compounds with the longest H-bond in each series (**1a** (0.990 Å), **2a** (0.991 Å), and **3b** (0.989 Å)) exhibited the shortest O−H bond length (0.987, 0.989, and 0.988 Å, respectively). The reason for this is the transfer of electron density from the nitrogen lone pair to the antibonding orbital σ^*_{O-H} of the acceptor OH group. Differences in this interaction are substituent-driven: electron-withdrawing substituents lower the ability of the nitrogen lone pair to donate electron density into the σ^*_{O-H} orbital, and hence the NO_2 derivatives in series **2** and **3** are the compounds with the weakest H-bonds because of the strong -I and -M effects of the NO_2 group.

Simultaneously, the bond angle C−O−H follows a similarly linear trend but of opposite direction: the compounds with the shortest H-bonds proved to have the smallest bond angles. In series **1**, the derivative with the weakest H-bond was **1a** (107.26°), whereas **1c** with the strongest H-bond in series **1** exhibited the smallest C−O−H bond angle (107.06°). In the other two series, the differences were even more distinct; in **2**, the difference between the derivatives with the weakest and the strongest H-bonds was 0.34146°, whereas in series **3**, it was 0.26238° (cf. Figure 8). This result unequivocally indicates that the OH group cumulatively tilts toward the nitrogen lone pair to advance its position to form effective intramolecular H-bonding. At the same time, the orbitals involved come into better positions for effective interaction and delocalization of the involved electron density. Whereas the slopes of the corresponding correlations for series **2** and **3** are parallel (influence of electronic substituent effects only), that for series **1** was different because of the different bulks of the alkyl substituents present.

The effects of the same substituents on other relevant bond lengths and bond angles were only minor or negligible. Only the steric effects of the substituents in series **1** deserve to be mentioned because the H···N−C angle proved to be dependent on the substituent volume (cf. Figure 8): with

TABLE 1: Selected Bond Lengths (angstroms) and Angles (deg) for the Aminonaphthol Derivatives (Calculated at the B3LYP/6-311+G(d,p) Level)

compound	substituent	C1−C2	C2−O3	O3−H4	C1−C6	C6−N5	N5−H4	C2−O3−H4	C1−C6−N4	H4−N5−C6
1e	Me	1.39321	1.35700	0.98900	1.52535	1.48841	1.76766	107.11723	110.36030	94.23982
1d	Pr	1.39335	1.35737	0.98894	1.52466	1.48865	1.77195	107.12531	109.89334	93.96328
1c	*i*-Pr	1.39388	1.35596	0.98982	1.52738	1.48863	1.75076	107.06168	110.67433	96.54481
1b	Et	1.39359	1.35713	0.98907	1.52481	1.48808	1.76905	107.09926	110.05630	94.02365
1a	H	1.39256	1.35730	0.98729	1.51682	1.48356	1.79880	107.25645	111.45789	91.29338
2g	*p*-Me	1.39297	1.35673	0.99091	1.52703	1.49578	1.74505	106.99729	110.67397	96.40689
2f	*p*-F	1.39294	1.35702	0.99028	1.52673	1.49491	1.75039	107.09415	110.64840	96.27542
2e	H	1.39298	1.35652	0.99043	1.52689	1.49528	1.74867	107.04072	110.71550	96.36611
2d	*p*-Br	1.39283	1.35721	0.98981	1.52706	1.49448	1.75236	107.12854	110.75101	96.33566
2c	*p*-OMe	1.39294	1.35683	0.99119	1.52784	1.49617	1.74220	106.96381	110.61694	96.44564
2b	*p*-Cl	1.39272	1.35710	0.98983	1.52685	1.49456	1.75115	107.13430	110.75335	96.39681
2a	*p*-NO_2	1.39298	1.35743	0.98890	1.52661	1.49284	1.75904	107.30527	110.86215	96.21004
3g	*p*-OMe	1.38990	1.35880	0.98943	1.52536	1.49235	1.78098	106.87004	110.45375	95.41885
3f	H	1.39007	1.35863	0.98897	1.52527	1.49148	1.78241	106.91998	110.57360	95.59876
3e	*p*-F	1.38995	1.35895	0.98873	1.52483	1.49120	1.78620	106.97783	110.45753	95.38498
3d	*p*-Br	1.38992	1.35905	0.98863	1.52508	1.49072	1.78428	106.99966	110.61518	95.56886
3c	*m*-Br	1.38999	1.35894	0.98846	1.52451	1.49029	1.78805	107.01803	110.60565	95.36588
3b	*m*-NO_2	1.38987	1.35979	0.98772	1.52438	1.48933	1.79452	107.13242	110.62205	95.26539
3a	*p*-Me	1.39003	1.35851	0.98921	1.52484	1.49198	1.78352	106.91358	110.46760	95.39819

increasing size of R, as expected, the (O)H···N−C angle was cumulatively enlarged with the compound with the longest H-bond (R = *i*-Pr) having the largest (O)H···N−C angle. In planar systems, the optimum value for this angle to form an intramolecular H-bond is 120°;[35] the wider the angle, the readier the formation of optimum H-bonds. In the studied sterically hindered, nonplanar systems **1**−**3**, the (O)H···N−C angle cannot achieve 120°, but the tendency is the same; the corresponding effect is compensated by the change in the dihedral angle C7−C1−C6−N5.

The calculated C1−C6 bond lengths also displayed a linear dependence on the H-bond length; mainly in series **1** with the alkyl substituents, this was caused by the steric effects. The bulkier the substituent and the shorter the H-bond, the longer the C1−C6 bond. Series **2** and **3** demonstrated minor variations in C1−C6, but the tendency was the same. For better H-bonding, the C1−C6 bond was longer.

Finally, the H-bond length in the Betti base derivatives was correlated to the substituent-induced ^{1}H chemical shifts (SCS) of the substituents R in **1**−**3** (cf. Figure 9); as expected, three different quite good correlations were obtained for the three series of compounds.

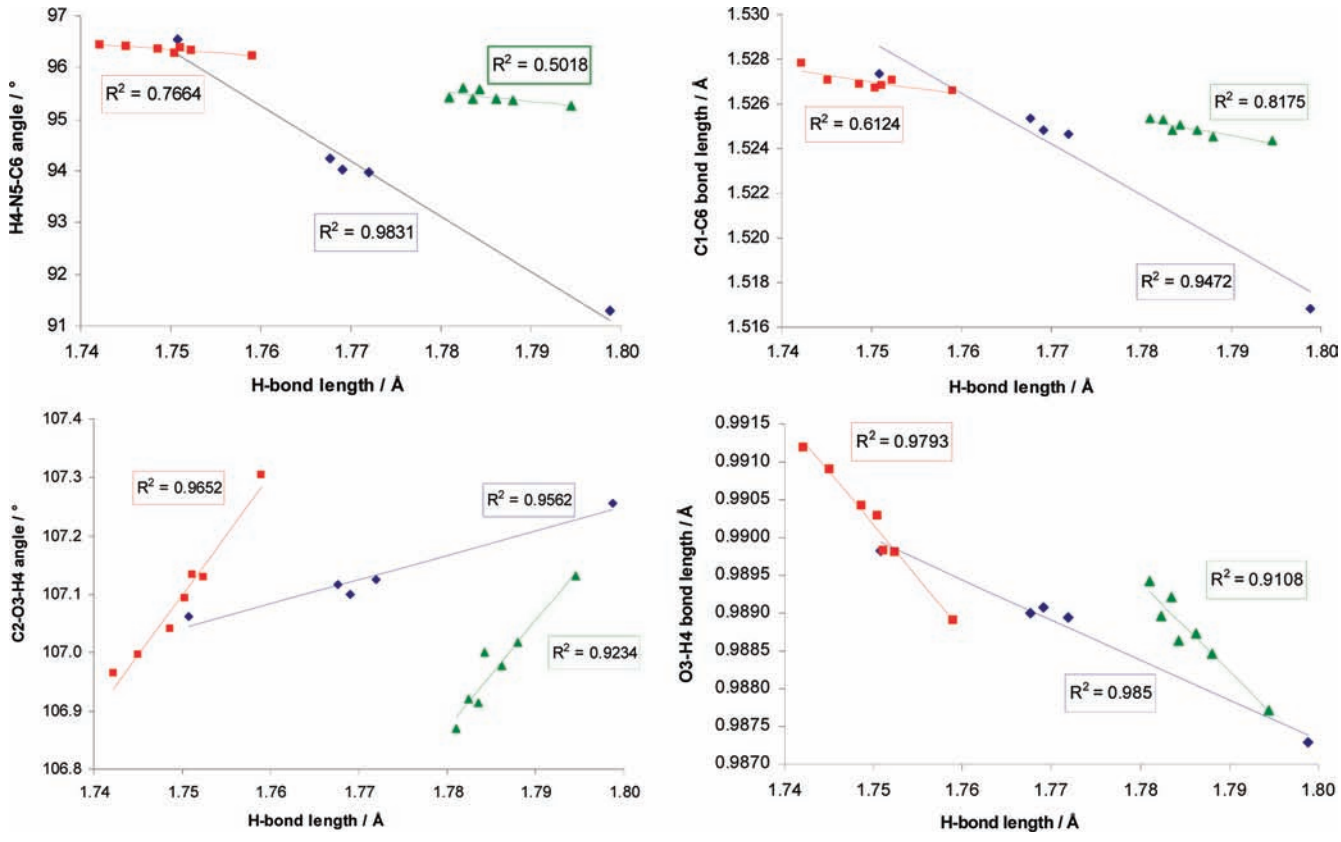

Figure 8. Various bond lengths and angles plotted versus H-bond length for series **1** (◆), series **2** (■), and series **3** (▲); regression coefficients are given.

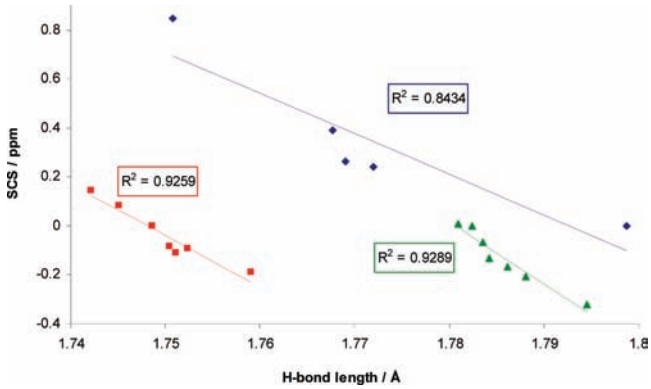

Figure 9. Cross-correlation of the SCSs in ppm versus the H-bond length in anstroms for series **1** (◆), series **2** (■), and series **3** (▲); linear regressions and their regression coefficients are to be seen.

TABLE 2: Hyperconjugation Energies ($n_N \rightarrow \sigma^*_{O-H}$) and OH···N H-bond lengths in Betti Base Derivatives 1−3

compound	substituent	energy/ kcal mol^{-1}	H-bond lengths/Å	occupancy LP(N)
1e	Me	22.47	1.76766	1.91566
1d	Pr	22.03	1.77195	1.91549
1c	*i*-Pr	23.72	1.75076	1.91362
1b	Et	22.28	1.76905	1.91506
1a	H	20.01	1.79880	1.92002
2g	*p*-Me	24.54	1.74505	1.91194
2f	*p*-F	24.00	1.75039	1.91270
2e	H	24.17	1.74867	1.91256
2d	*p*-Br	23.80	1.75236	1.91311
2c	*p*-OMe	24.84	1.74220	1.91127
2b	*p*-Cl	23.89	1.75115	1.91300
2a	*p*-NO_2	23.06	1.75904	1.91447
3g	*p*-OMe	21.96	1.78098	1.91340
3f	H	21.79	1.78241	1.91393
3e	*p*-F	21.41	1.78620	1.91428
3d	*p*-Br	21.53	1.78428	1.91418
3c	*m*-Br	21.22	1.78805	1.91474
3b	*m*-NO_2	20.66	1.79452	1.91534
3a	*p*-Me	21.69	1.78352	1.91401

3.4. NBO Analysis (Search for Predominant Hyperconjugative Interactions). As regards the global minimum structures of the Betti base derivatives **1**−**3**, NBO calculations were performed to determine the contributing and predominant orbital interactions responsible for the intramolecular H-bonding. As the main hyperconjugative interaction, the $n_N \rightarrow \sigma^*_{O-H}$ interdependence was identified, which was previously assigned as the major contribution to the H-bond.[36]

The geometries of the most stable conformers of the derivatives in series **1**−**3** are depicted in Figure 10. From these fully optimized structures, the H-bond distances O−H···N between the nitrogen and the OH hydrogen were measured to be between 1.7 and 1.8 Å and are given in Table 2.

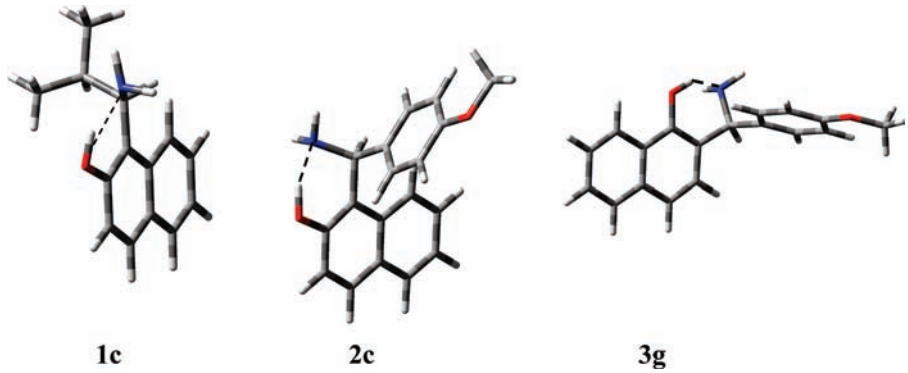

Figure 10. Optimized structures with the shortest H-bond for each series.

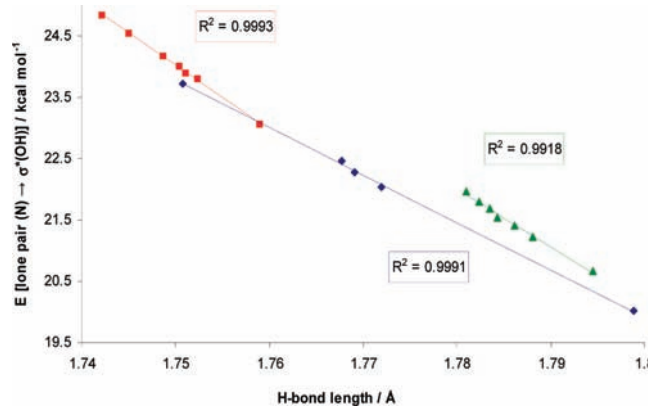

Figure 11. Cross-correlation between hyperconjugation energy *E* and H-bond length for series **1** (◆), series **2** (■), and series **3** (▲).

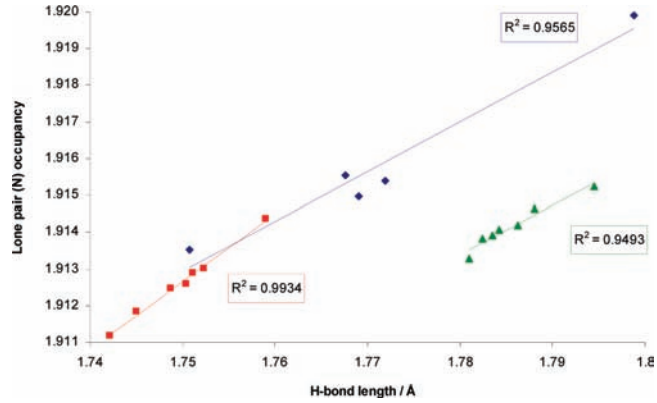

Figure 12. Cross-correlations of the occupancy of the nitrogen lone pair versus the H-bond length for series **1** (◆), series **2** (■), and series **3** (▲); linear regressions were obtained and regression coefficients are given.

Table 2 also reports the complete hyperconjugation stabilization energies obtained from the second-order perturbation theory analysis of the Fock matrix by NBO analysis; the values ranged between 20.01 and 24.84 kcal mol^{-1} (cf. Table 2).

Consideration of this set of values indicates the importance of this hyperconjugative interaction as the fundamental cause of H-bonding: In series **1**, the *i*-Pr derivative contained the shortest H-bond (1.751 Å) and the highest hyperconjugation stabilization energy (23.72 kcal mol^{-1}). In series **2**, the shortest H-bond (1.742 Å) and the highest hyperconjugation stabilization energy (24.84 kcal mol^{-1}) were those for the OMe derivative

TABLE 3: Hammett Constants, σ, for Substituents, R, in 1−3

compound	substituent	Hammett constant[22]
1c	*i*-Pr	−0.15
1e	Me	−0.17
1b	Et	−0.15
1d	Pr	−0.13
1a	H	0
2c	*p*-OMe	−0.27
2g	*p*-Me	−0.17
2e	H	0
2f	*p*-F	0.06
2b	*p*-Cl	0.23
2d	*p*-Br	0.23
2a	*p*-NO_2	0.78
3g	*p*-OMe	−0.27
3f	H	0
3a	*p*-Me	−0.17
3d	*p*-Br	0.23
3e	*p*-F	0.06
3c	*m*-Br	0.39
3b	*m*-NO_2	0.71

2c. Finally, in series **3**, it was again the OMe derivative (**3g**) that had the shortest H-bond (1.781 Å) and the highest hyperconjugation stabilization energy (21.96 kcal mol^{-1}). The cross-correlation of the H-bond length with the hyperconjugation stabilization energy revealed excellent correlations with R^2 of 0.9918 for series **1**, 0.9991 for series **3**, and 0.9993 for series **2** (cf. Figure 11); shorter distances were accompanied by higher hyperconjugative stabilization. Therefore, hyperconjugative stabilization energies $n_N \rightarrow \sigma^*_{O-H}$ alone can furnish reliable information on the strength of H-bonding present.

In series **1**, the difference between the weakest and strongest H-bonds was much larger than that in series **2** and **3**, for which the hyperconjugative stabilization energy differences were 3.71 (in series **1**), 1.78 (in series **2**), and 1.3 kcal mol^{-1} (in series **3**). There is only one explanation for this observation: the bulky substituents in series **1** are positioned closer to the H-bond and, under the influence the steric substituent effect, determine both the strength and the length of the incorporated intramolecular H-bonds much more effectively than do the substituents in series **2** and **3**. Furthermore, the latter affect the H-bonds by electronic substituent effects only, which, as concerns H-bonding, are obviously much weaker than the steric influences in series **1**. However, as mentioned earlier, the electronic substituent effects in series **2** and **3** are comparable.

The critical analysis of the occupancy of the nitrogen lone pair as the electron donor pointed to the same tendency: the shorter the H-bond, the lower the occupancy of this lone pair, which is congruent with a shift of the electron density toward the σ^*_{O-H} orbital for more effective intramolecular H-bonding (cf. Figure 12).

Figures 11 and 12 show the absolute differences between this intramolecular H-bonding in systems **2** and **3**. The analogues in series **3** proved to have the longest intramolecular H-bonds even though the substituents were nearly the same in both series. Comparison of the *p*-OMe derivatives in each series demonstrates that the occupancy of the nitrogen lone pair is 0.0213 higher in **3g** than in **2c**, and the corresponding hyperconjugative stabilization is 2.88 kcal mol^{-1} larger in **2c** (cf. Table 2). Differences in the substituent effect on the intramolecular H-bonding in **2** and **3** can be concluded.

3.5. Substituent Constants to Quantify Electronic Effects of Substituents on the Strength of Intramolecular H-Bonding. A well-known possibility to examine the electronic effect of a substituent X is the use of the Hammett equation and the corresponding Hammett substituent constant σ.

$$\sigma = \log K_x - \log K_H \qquad (2)$$

The values of σ were determined by Hammett from the ionization constants of benzoic acids. K_H is the ionization constant of benzoic acid in water at 25 °C, and K_X is the corresponding constant for a *m*- or *p*-substituted benzoic acid under the same experimental conditions.[22a] Positive values of σ indicate electron withdrawal by the substituents from the aromatic ring, whereas negative σ values indicate electron release.[22b] The available substituent constants, σ (Table 3), for the Betti base substituents, R, were correlated to the corresponding lengths of the intramolecular H-bonds in series **1**−**3**; the corresponding correlations are given in Figure 13.

The best correlation was obtained for the substituents in series **2**: the H-bond strength decreased, as in series **3**, but with a lower correlation quotient in the sequence *p*-OMe > *p*-Me > H > *p*-F > *p*-Cl > *p*-Br > *p*-NO_2 in complete agreement with the Hammett constants. Electron-releasing substituents favor intramolecular H-bonding, whereas electron-withdrawing substituents such as NO_2 lower the electron density at the aromatic system and hence the ability of the nitrogen to transfer lone pair electron density to the antibonding σ^*_{O-H} orbital of the OH group. As mentioned above, the correlation for series **3** was not so strong, but the slope of the correlation was similar to that in series **2**, which

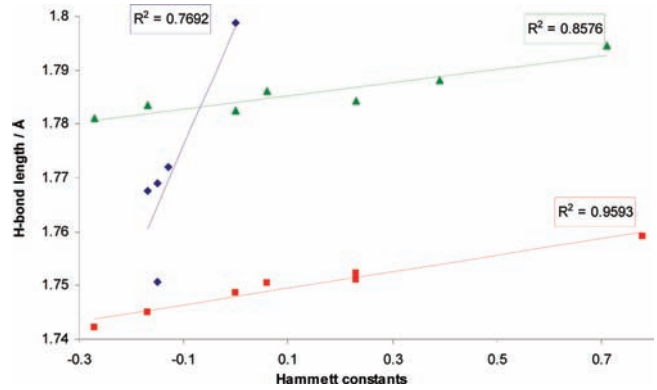

Figure 13. Plot of the Hammett constants versus the H-bond distance for series **1** (◆), series **2** (■), and series **3** (▲); regression lines and regression coefficients are given.

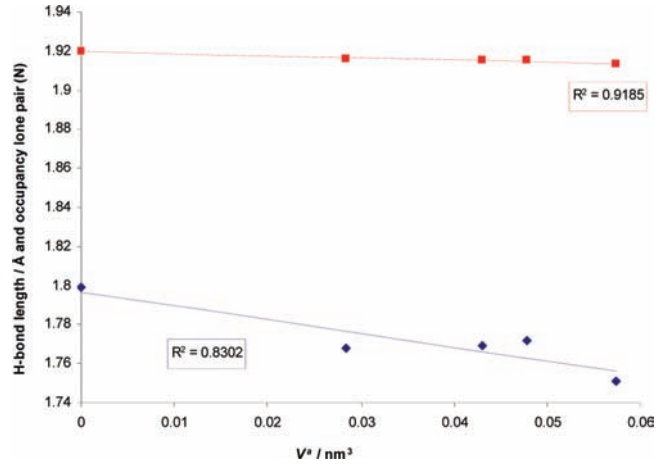

Figure 14. Correlations of the Meyer parameters (V^a in cubic nanometers per molecule) with the H-bond length (◆) and the occupancy of the nitrogen lone pair (■).

confirms the same influence of the substituents on the intramolecular H-bonds present.

Finally, there is obviously almost no slope in the correlation for series **1**, where steric substituent effects strongly influence the H-bonding. Nevertheless, Hammett substituent constants, σ, increased slightly in the sequence H < Me < Et < Pr < *i*-Pr. The corresponding correlation was the weakest of those for series **1**−**3** but was clear-cut. Therefore, in addition to the predominant bulk effect of substituents R in series **1**, there is a small electronic substituent effect that acts in the same direction as the latter. However, the steric effect is much greater, and the corresponding electronic effect can almost be neglected. Both the H-bond length and the occupation of the nitrogen lone pair were correlated with Meyer's substituent parameters[21] in Figure 14, which relate to the steric effects of the substituents. The correlations were not very strong, but, in particular, that of the nitrogen lone pair versus V^a proves that the steric effects of the substituents predominate in the structural variations in the series **1** compounds.

4. Conclusions

Three series of 1,3-amino α- and β-naphthols (**1**−**3**) were studied with respect to inter/intramolecular O−H···N or N−H···O H-bonding. Both experimentally (by NMR spectroscopy) and computationally at the DFT level of theory, the existence of only O−H···N intramolecular H-bonding was unequivocally identified. The strength of the intramolecular H-bond, which is dominated by $n_N \rightarrow \sigma^*_{O-H}$ hyperconjugation, proved to be dependent on the steric and electronic effects of the substituents R in **1**−**3**: electron-withdrawing substituents reduced the ability of the nitrogen lone pair to donate electron density to the σ^*_{O-H} orbital and hence the strength of the H-bond. The lengths of the O−H and C1−C6 bonds, the bond angle C−O−H, the angle (O)H···N−C and the dihedral angle C7−C1−C6−N5 change in agreement with the effects of the substituents. Electronic substituent effects were identified and quantified via the correlations of the H-bond lengths versus the Hammett substituent constants, σ; the intramolecular H-bonds in series **1** are additionally determined by the steric effects of substituents, R.

Supporting Information Available: *x*,*y*,*z*-Coordinates and absolute energies at the B3LYP/6-311+G(d,p) level of theory for **1**−**3**. This material is available free of charge via the Internet at http://pubs.acs.org.

References and Notes

(1) Schuster, I. I. *J. Chem. Soc., Perkin Trans. 2* **2002**, 1961–1966.
(2) Dias, L. C.; Ferreira, A. B.; Tormena, C. F. *J. Phys. Chem. A* **2008**, *112*, 232–237.
(3) Winstanley, K. J.; Smith, D. K. *J. Org. Chem.* **2007**, *72*, 2803–2815.
(4) Schuster, P.; Wolschann, P. *Chem. Mon.* **1999**, *130*, 947–960.
(5) Petterson, K. A.; Stein, R. S.; Drake, M. D.; Roberts, J. D. *Magn. Reson. Chem.* **2005**, *43*, 225–230.
(6) (a) Afonin, A. V.; Ushakov, I. A.; Mikhaleva, A. I.; Trofimov, B. A. *Magn. Reson. Chem.* **2007**, *45*, 220–230. (b) Afonin, A. V.; Ushakov, I. A.; Sobenina, L. N.; Stepanova, Z. V.; Trofimov, B. A. *Magn. Reson. Chem.* **2006**, *44*, 59–65.
(7) Foti, M. C.; DiLabio, G. A.; Ingold, K. U. *J. Am. Chem. Soc.* **2003**, *125*, 14642–14647.
(8) Misic-Vulkovc, M.; Jovanovic, S.; Mijin, D.; Csanadi, J.; Djokovic, D. *J. Serb. Chem. Soc.* **2007**, *72*, 1229–1236.
(9) Vinogradov, S. N.; Linnell, R. H. *Hydrogen Bonding*; Van Nostrand Reinhold: New York, 1971.
(10) Pinjari, R. V.; Joshi, K. A.; Gejji, S. P. *J. Phys. Chem. A.* **2007**, *111*, 13583–13589.
(11) (a) Freitas, M. P.; Tormena, C. F.; Rittner, R. *J. Mol. Struct.* **2001**, *570*, 175. (b) Freitas, M. P.; Tormena, C. F.; Rittner, R.; Abraham, R. J. *J. Phys. Org. Chem.* **2003**, *16*, 27.
(12) Bernet, B.; Vasella, A. *Helv. Chim. Acta* **2007**, *90*, 1874–1888.
(13) Aguilar-Castro, L.; Tlahuextl, M.; Mendoza-Huizar, L. H.; Tapia-Benavides, A. R.; Tlahuext, H. *Arkivoc* **2008**, *v*, 210–226.
(14) Glendening, E. D.; Badenhoop, J. K.; Reed, A. E.; Carpenter, J. E.; Bohmann, J. A.; Morales, C. M.; Weinhold, F. *NBO 5.0*; Theoretical Chemistry Institute, University of Wisconsin: Madison, WI, 2001.
(15) Ducati, L. C.; Freitas, M. P.; Tormena, C. F.; Rittner, R. *THEOCHEM* **2008**, *851*, 147–157.
(16) De Oliveira, P. R.; Rittner, R. *Spectrochim. Acta, Part A* **2008**, *70*, 1079–1086.
(17) Tóth, D.; Szatmári, I.; Fülöp, F. *Eur. J. Org. Chem.* **2006**, 4664–4669.
(18) Szatmári, I.; Martinek, T. A.; Lázár, L.; Fülöp, F. *Tetrahedron* **2003**, *59*, 2877–2884.
(19) Szatmári, I.; Martinek, T. A.; Lázár, L.; Fülöp, F. *Eur. J. Org. Chem.* **2004**, 2231–2238.
(20) Desai, N. C.; Shukla, H. K.; Langalia, N. A.; Thaker, K. A. *J. Ind. Chem. Soc.* **1984**, *61*, 711–713.
(21) Meyer, A. Z. *J. Chem. Soc., Perkin Trans. 2* **1986**, 1567–1986.
(22) (a) Hansch, C.; Leo, A.; Taft, R. W. *Chem. Rev.* **1991**, *91*, 165–195. (b) Hansch, C.; Leo, A. *Substituent Constants for Correlation Analysis in Chemistry and Biology*; Wiley-Interscience: New York, 1978.
(23) Paul, H.-H.; Sapper, H.; Lohmann, W. *Biochem. Pharmacol.* **1980**, *29*, 137–140.
(24) Frisch, M. J.; Trucks, G. W.; Schlegel, H. B.; Scuseria, G. E.; Robb, M. A.; Cheeseman, J. R.; Montgomery, J. A., Jr.; Vreven, T.; Kudin, K. N.; Burant, J. C.; Millam, J. M.; Iyengar, S. S.; Tomasi, J.; Barone, V.; Mennucci, B.; Cossi, M.; Scalmani, G.; Rega, N.; Petersson, G. A.; Nakatsuji, H.; Hada, M.; Ehara, M.; Toyota, K.; Fukuda, R.; Hasegawa, J.; Ishida, M.; Nakajima, T.; Honda, Y.; Kitao, O.; Nakai, H.; Klene, M.; Li, X.; Knox, J. E.; Hratchian, H. P.; Cross, J. B.; Bakken, V.; Adamo, C.; Jaramillo, J.; Gomperts, R.; Stratmann, R. E.; Yazyev, O.; Austin, A. J.; Cammi, R.; Pomelli, C.; Ochterski, J. W.; Ayala, P. Y.; Morokuma, K.; Voth, G. A.; Salvador, P.; Dannenberg, J. J.; Zakrzewski, V. G.; Dapprich, S.; Daniels, A. D.; Strain, M. C.; Farkas, O.; Malick, D. K.; Rabuck, A. D.; Raghavachari, K.; Foresman, J. B.; Ortiz, J. V.; Cui, Q.; Baboul, A. G.; Clifford, S.; Cioslowski, J.; Stefanov, B. B.; Liu, G.; Liashenko, A.; Piskorz, P.; Komaromi, I.; Martin, R. L.; Fox, D. J.; Keith, T.; Al-Laham, M. A.; Peng, C. Y.; Nanayakkara, A.; Challacombe, M.; Gill, P. M. W.; Johnson, B.; Chen, W.; Wong, M. W.; Gonzalez, C.; Pople, J. A. *Gaussian 03*, revision C.02; Gaussian, Inc.: Wallingford, CT, 2004.
(25) Becke, A. D. *J. Chem. Phys.* **1993**, *98*, 5648–5652.
(26) Lee, C.; Yang, W.; Parr, R. G. *Phys. Rev. B* **1988**, *37*, 785–789.
(27) Ditchfield, R.; Hehre, W. J.; Pople, J. A. *J. Chem. Phys.* **1971**, *54*, 724–728.
(28) Weinhold, F. *NBO 5.0 Program Manual: Natural Bond Orbital Analysis Programs*; Theoretical Chemistry Institute, University of Wisconsin: Madison, Wisconsin, 2001.
(29) Wolinski, K.; Hinton, J. F.; Pulay, P. *J. Am. Chem. Soc.* **1990**, *112*, 8251–8260.
(30) Lomas, J. S.; Adenier, A.; Cordier, C.; Lacroix, J.-C. *J. Chem. Soc., Perkin Trans. 2* **1998**, 2647–2652.
(31) Gellman, S. H.; Dado, G. P.; Liang, G. B.; Adams, B. R. *J. Am. Chem. Soc.* **1991**, *113*, 1164–1173.
(32) Bernet, B.; Vasella, A. *Helv. Chim. Acta* **2000**, *83*, 995–1021.
(33) Muddasani, P. R.; Bozo, E.; Bernet, B.; Vasella, A. *Helv. Chim. Acta* **1994**, *77*, 257–263.
(34) Kessler, H. *Angew. Chem., Int. Ed. Engl.* **1982**, *21*, 512–523.
(35) Shchavlev, A. E.; Pankratov, A. N.; Enchev, V. *J. Phys. Chem. A.* **2007**, *111*, 7112–7123.
(36) Reed, A. E.; Curtiss, L. A.; Weinhold, F. *Chem. Rev.* **1988**, *88*, 899–926.

JP902731N